Postnatal development of mouse heart: formation of energetic microdomains

Jérôme Piquereau[1,2], Marta Novotova[3], Dominique Fortin[1,2], Anne Garnier[1,2], Renée Ventura-Clapier[1,2], Vladimir Veksler[1,2] and Frédéric Joubert[1,2]

[1] *INSERM, U-769, F-92296 Châtenay-Malabry, France*
[2] *Univ Paris-Sud, IFR141, F-92296 Châtenay-Malabry, France*
[3] *Institute of Molecular Physiology & Genetics, Slovak Academy of Sciences, Bratislava, Slovak Republic*

Cardiomyocyte contractile function requires tight control of the ATP/ADP ratio in the vicinity of the myosin-ATPase and sarcoplasmic reticulum ATPase (SERCA). In these cells, the main systems that provide energy are creatine kinase (CK), which catalyses phosphotransfer from phosphocreatine to ADP, and direct adenine nucleotide channelling (DANC) from mitochondria to ATPases. However, it is not known how and when these complex energetic systems are established during postnatal development. We therefore studied the maturation of the efficacy with which DANC and CK maintain ATP/ADP-dependent SR and myofibrillar function (SR Ca^{2+} pumping and prevention of rigor tension), as well as the maturation of mitochondrial oxidative capacity. Experiments were performed on saponin-skinned fibres from left ventricles of 3-, 7-, 21-, 42- and 63-day-old mice. Cardiomyocyte and mitochondrial network morphology were characterized using electron microscopy. Our results show an early building-up of energetic microdomains in the developing mouse heart. CK efficacy for myosin-ATPase regulation was already maximal 3 days after birth, while for SERCA regulation it progressively increased until 21 days after birth. Seven days after birth, DANC for these two ATPases was as effective as in adult mice, despite a non-maximal mitochondrial respiration capacity. However, 3 days after birth, DANC between mitochondria and myosin-ATPase was not yet fully efficient. To prevent rigor tension in the presence of working mitochondria, the myosin-ATPase needed more intracellular MgATP in 3-day-old mice than in 7-day-old mice ($pMgATP_{50}$ 4.03 ± 0.02 and 4.36 ± 0.07, respectively, $P < 0.05$), whereas the intrinsic sensitivity of myofibrils to ATP (when mitochondria were inhibited) was similar at both ages. This may be due to the significant remodelling of the cytoarchitecture that occurs between these ages (cytosolic space reduction, formation of the mitochondrial network around the myofibrils). These results reveal a link between the maturation of intracellular energy pathways and cell architecture.

(Received 9 March 2010; accepted after revision 14 March 2010; first published online 17 May 2010)
Corresponding author F. Joubert: U-769 INSERM, Faculté de Pharmacie, Université Paris-Sud, 5 rue J-B Clément, 92296 Châtenay-Malabry, France. Email: frederic.joubert@u-psud.fr

Abbreviations ACR, acceptor control ratio; Cr, creatine; CK, creatine kinase; DANC, direct adenine nucleotide channelling; mi-CK, mitochondrial creatine kinase; MM-CK, cytosolic muscle creatine kinase isoform; MHC, myosin heavy chain; PCr, phosphocreatine; SERCA, sarcoplasmic reticulum Ca^{2+}-ATPase; SR, sarcoplasmic reticulum.

Introduction

Cardiomyocytes are highly specialized and organized cells. The contractile function of these cells requires a high local ATP/ADP ratio in the vicinity of the sarcoplasmic reticulum (SR) Ca^{2+}-ATPase (SERCA) and myosin-ATPase, in order to drive calcium loading and force development, respectively (Ventura-Clapier *et al.* 1998). Thus, the main energy consumers of the cardiac cell are localized in the SR and myofibrillar compartments, while energy production is mainly performed by the mitochondria. Obviously, this energy must be quickly and efficiently transferred from the mitochondria to the ATPases according to demand, in order to ensure an optimal energetic microenvironment in the vicinity of these energy consumers.

There are two main intracellular energy pathways that are currently known in adult cardiomyocytes (Fig. 1). The

 DOI: 10.1113/jphysiol.2010.189670

first is the creatine kinase (CK) system, which catalyses the reversible transfer of a high energy phosphate group from ATP to creatine (Cr). This system relies on the presence of mitochondrial CK (mi-CK) bound to the outer surface of the inner mitochondrial membrane, and the presence of a cytosolic muscle CK isoform (MM-CK) bound to myofilaments and SR close to the ATPases. mi-CK transfers the phosphate group from ATP generated in the mitochondria to Cr, thereby producing phosphocreatine (PCr), which diffuses to the energy-consuming sites. Creatine kinase bound to the myofilaments and the SR rephosphorylates locally produced ADP by using PCr (for reviews see Wallimann *et al.* 1992; Saks *et al.* 1994; Ventura-Clapier & Veksler 1994).

The second energy pathway is direct adenine nucleotide channelling (DANC) between mitochondria and ATPases, which occurs independently of cytosolic and bound CK (Kaasik *et al.* 2001; Seppet *et al.* 2001). The close proximity of mitochondria and ATPases, and the juxtaposition of mitochondria, SR and myofilaments, probably promotes efficient DANC. Indeed, adult cardiomyocytes exhibit a sophisticated subcellular architecture in which large mitochondria are strictly ordered between rows of contractile proteins (Ogata & Yamasaki 1985) and are specifically arranged with the SR and myofilaments into intracellular energetic units (Saks *et al.* 2001; Seppet *et al.* 2005). Thus, this highly specialized architecture of the cardiomyocyte, and also its cytoskeleton, which is responsible for the structural organisation, could be a key requirement for optimal energy transfer. Previous studies in our laboratory on the MLP- and desmin-null mouse heart, in which there is cytoskeletal remodelling and mitochondria disorganization, showed that direct ATP/ADP channelling between mitochondria and SERCA was altered, suggesting that cytoarchitectural perturbation could have a direct effect on this energetic system (Wilding *et al.* 2006).

It is generally accepted that perinatal development of cardiomyocytes is associated with a profound reorganization of the cell architecture involving an increase in mitochondrial and myofibrillar mass and SR maturation. Postnatal growth of the mouse heart is divided into three different phases (Leu *et al.* 2001): hyperplasia (until postnatal day 4), rapid hypertrophy (between days 5 and 15) and slow hypertrophy (from day 15 onwards). It seems likely that any major modification of the energetic signalling that may occur would therefore take place during the first two stages of development.

Thus, it is reasonable to suggest that such developmental changes in cytoarchitecture result in the formation of the energetic microdomains very early in postnatal life. However, the process of energy pathway maturation is still poorly understood. A detailed study of the evolution of energetic microdomains during postnatal development could allow us to understand their function much better. Moreover, perinatal development of cardiac energy metabolism has been investigated mostly in the rat, rabbit and guinea pig (for review see Hoerter *et al.* 1994; Ostadal *et al.* 1999; Hew & Keller 2003), but not the mouse, the species most widely used today for studying the effects of genetic manipulation on the heart. The aim of the present study was therefore to correlate developmental changes in the efficacy of the different energetic pathways with the profound reorganisation of cellular ultrastructure that occurs during this period (Leu *et al.* 2001).

Methods

Animals

Mice (strain C57Bl6) of different ages (3, 7, 21, 42 and 63 days) were anaesthetized by intraperitoneal injection of pentobarbital (60 mg kg^{-1}). This procedure complied with the recommendations of the institutional animal care and use committee of INSERM. After thoracotomy, hearts were excised and rinsed in ice-cold calcium free Krebs solution equilibrated with 95%O_2–5%CO_2. A part of each left ventricle was immediately frozen in liquid nitrogen for further biochemical determinations and another part was taken in order to prepare cardiac muscle fibres for the mechanical and respiration experiments. For measurements of SR and myofibrillar function, papillary muscle fibres were dissected and permeabilized for 30 min in saponin (50 μg.ml^{-1}), as described previously (De Sousa *et al.* 1999; Kaasik *et al.* 2001). For mitochondrial function measurements, muscle fibres were dissected from the endocardial surface of the left ventricle (Kaasik *et al.* 2001).

Estimation of SR calcium uptake

The contribution of the different energetic systems to the provision of ATP for SERCA function was estimated by measuring SR calcium after loading under various energetic conditions as previously described (Minajeva *et al.* 1996; Wilding *et al.* 2006). Permeabilized muscle fibres were mounted on a device equipped with a force transducer which recorded the tension developed by the muscle fibres (Ventura-Clapier *et al.* 1995). Calcium uptake for 5 min at pCa 6.5 occurred in the presence of exogenous ATP, with or without endogenous mitochondrial ATP production and/or activation of the CK system (Fig. 1). To estimate the amount of calcium pumped by the SR, calcium release was elicited with 5 mmol l^{-1} caffeine, and was detected using the resulting contractile force transient. Although different energetic loading conditions were tested, calcium release was always measured using the same solution, which provided exogenous ATP, and mitochondrial and

CK-system activation together. By relating the subsequent contractile force elicited with caffeine to the pCa–tension relationship, which was determined for each muscle fibre, the $[Ca^{2+}]$–time integral was calculated and used as an index of SR calcium load (Minajeva *et al.* 1996; Kaasik *et al.* 2001). The ATP channelling solution (DANC) contained (in mmol l^{-1}): EGTA 10 (0.2 during calcium release), Bes, 40 (pH 7.1), free Mg^{2+} 1, taurine 20, glutamic acid 10, malic acid 4, K_2HPO_4 3, dithiothreitol 0.5, P^1,P^5-diadenosine pentaphosphate 0.04 (to inhibit adenylate kinase activity), and MgATP 3.16; ionic strength was adjusted to 160 mmol l^{-1} with potassium methanesulfonate, and 6% dextran was added to maintain normal cell volume. Addition of 12 mmol l^{-1} PCr to this solution caused SR loading supported by DANC and the bound CK system together (DANC+CK, optimal energetic conditions). Loading supported by the CK system only was achieved by adding 2 mmol l^{-1} sodium azide, which blocked mitochondrial respiration. Addition of 2 mmol l^{-1} azide in the absence of PCr caused SR loading supported by exogenous ATP only.

Estimation of the myofibrillar function

The pMgATP–rigor tension relation of saponin-permeabilized muscle fibres was used for studying the ability of the different energetic systems to supply ATP for myosin-ATPase function. Under each energetic condition the pMgATP–rigor tension relationship was estimated by progressively decreasing ATP concentration under isometric conditions (Ventura-Clapier *et al.* 1995). Rigor tension is a tension developed when the MgATP concentration in the vicinity of the myofibrillar ATPase is not sufficient to ensure the dissociation of myosin heads from the actin filament. This effect is enhanced by the presence of ADP (Ventura-Clapier & Veksler 1994), and thus rigor tension is a good index of the ATP/ADP ratio in the vicinity of myosin ATPase. Data were fitted using the Hill equation: $T = K/(K + [\mathrm{MgATP}]^{n_H})$, where T is the relative rigor tension, K a constant, and n_H the Hill coefficient. This fitting procedure was used to calculate $pMgATP_{50}$, which is the negative logarithm of [MgATP] at which half-maximum rigor tension is obtained. The solutions used were the same as the solutions used for the estimation of SR calcium uptake, except for the ATP concentration, which varied in this experiment.

Analysis of *in situ* mitochondrial function

The respiration rate of the mitochondrial population in saponin-permeabilized muscle fibres was determined using a Clark electrode (Strathkelvin Instruments, North Lanarkshire, Scotland, UK) as previously described (Veksler *et al.* 1987; Kuznetsov *et al.* 2008). A protocol was designed to determine the sensitivity of the mitochondrial respiration to external ADP and creatine. Bundles of muscle fibres were transferred to an oxygraphic cell at 22°C in which there was a respiration solution containing (in mmol l^{-1}): EGTA-CaEGTA buffer 10 (free Ca^{2+} 0.1), free Mg^{2+} 1, dithiothreitol 0.5, imidazole 20, taurine 20, glutamate 10, malate 4, K_2HPO_4 3, fatty acid free bovine serum albumin (2 mg ml^{-1}), with ionic strength adjusted to 160 by addition of potassium methanesulfonate. The basal respiration rate of mitochondria in the absence of ADP (V_0) was determined, then respiration was stimulated by the addition of a submaximal ADP concentration (0.1 mmol l^{-1}). After a few minutes, 12 mmol l^{-1} creatine was added to the chamber and finally the maximal respiration rate (V_{max}) was measured by adding saturating [ADP] (2 mmol l^{-1}). Given that the respiration rate depends on [ADP] according to the Michaelis–Menten law, the apparent K_m values in the presence and absence of creatine were calculated using the equation $K_m = 100\ \mu M \times (V_{max}/V_{100} - 1)$, where V_{100} is the respiration rate at 100 μmol l^{-1} ADP.

The acceptor control ratio (ACR) was calculated as V_{max}/V_0. After each respiration experiment, the bundles of muscle fibres were removed from the oxygraphic cell and dried and weighed so that respiration rates could be expressed in μmol O_2 min^{-1} (g dry weight)$^{-1}$.

Biochemical analysis

Frozen tissues were homogenized in buffer (50 mg ml^{-1}) containing (in mmol l^{-1}) Hepes 5, EGTA 1, DTT 1 and 0.1% Triton X-100 and incubated for 1 h at 0°C for complete enzyme extraction. Activities of total CK, citrate synthase and mitochondrial complex I were measured

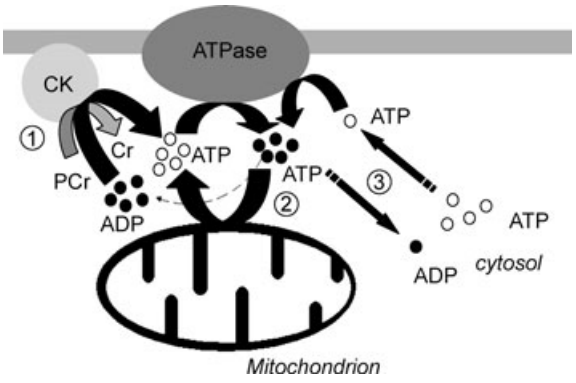

Figure 1. Pathways of energy supply for ATPases in the cardiomyocyte
1, creatine kinase (CK) bound to the myofilaments or the SR rephosphorylates locally produced ADP at the expense of PCr. 2, the juxtaposition of the mitochondrion and ATPase allows for direct adenine nucleotide channelling (DANC). 3, adenine nucleotides in the neighbourhood of ATPase exchange with those in the bulk of cytosol via diffusion.

using standard spectrophotometric assays (Wharton & Tzagoloff 1967; Estornell *et al.* 1993; Veksler *et al.* 1995; Ventura-Clapier *et al.* 1995).

Western blot

Protein extracts from hearts of mice of different ages were separated on SDS-polyacrylamide gel (8% for SERCA2, 12% for phospholamban, calsequestrin and mi-CK) and then transferred to nitrocellulose membranes. After 1 h of blocking with milk, the membranes were incubated overnight with primary antibody (SERCA2: cat no. 8094, Santa Cruz Biotechnology, Inc. (Santa Cruz, CA, USA) produced in goat; phospholamban: cat no. 05-205, Upstate Biotechnology (Lake Placid, NY, USA), produced in mouse; calsequestrin: cat no. PA1-913, Thermo Fisher Scientific (Rockford, IL, USA), produced in rabbit; mi-CK: a kind gift of Drs Z. Khuchua and W. Quin, Washington University, St Louis, MO, USA, produced in rabbit). After washing, the membranes were incubated with a secondary antibody for 1 h and visualised using chemiluminescent substrate (SuperSignal West Dura kit, Thermo Fisher Scientific). Light emission was detected by autoradiography and quantified using an image-analysis system (Bio-Rad). The antibodies used were highly specific because only one band of the appropriate size (SERCA2: 110 kDa, phospholamban: 25 kDa, calsequestrin: 55 kDa, mi-CK: 43 kDa) was obtained each time.

Real-time quantitative PCR analysis

Total cardiac RNA was extracted using standard procedures. Oligo-dT first strand cDNA was synthesized from 5 μg total RNA using superscript II reverse transcriptase (Invitrogen). Real-time RT-PCR was performed using the SYBR Green method on a LightCycler rapid thermal cycler (Roche Diagnostics, Indianapolis, IN, USA) as previously described (Garnier *et al.* 2003). The following primers were used: α-MHC, forward primer CCAATGAGTACCGCGTGAA, reverse primer ACAGTCATGCCGGGATGAT; β-MHC, forward primer, ATGTGCCGGACCTTGGAA, reverse primer, CCTCGGGTTAGCTGAGAGATCA; TATA box binding protein (TBP), forward primer, GGCCTCTCAGAAGCATCACTA, reverse primer, GCCAAGCCCTGAGCATAA; glyceraldehyde 3-phosphate dehydrogenase (GAPDH), forward primer, TGCACCACCAACTGCTTAG, reverse primer, GATGCAGGGATGATGTTC. Amplification was allowed to proceed for 30–40 cycles, each consisting of denaturation (95°C, 10 s), annealing at specific temperature of 55°C for TBP, 58°C for α- and β-MHC and 60°C for GAPDH for 5 s, and extension at 72°C for 7–10 s depending on the length of the PCR product (25 bp per second). mRNA levels for all target genes were normalized to TBP and GAPDH levels using GeNorm software (Vandesompele *et al.* 2002).

Electron microscopy and stereological experiments

Samples of mouse left ventricular papillary muscle ($n = 3$–5 for the different ages) were prepared for electron microscopy as previously described (Wilding *et al.* 2006). Ultrathin (60–65 nm) longitudinal sections were contrasted with lead citrate and studied using a JEM 1200 (JEOL, Tokyo, Japan) electron microscope. Images were recorded using a Gatan Dual Vision 300W CCD camera (Gatan Inc., Pleasanton, CA, USA).

Stereological analysis

The sections were cut from each tissue block at two randomly selected levels separated by more than 50 μm. Five micrographs taken at a magnification of 7500× from each section were obtained. Twenty pictures were analysed from 2 hearts for each group.

The volume density of mitochondria, myofilaments, cytoplasm and lipid drops were estimated using ImageJ software. A grid in which each line intersection serves as a sample point was generated on each image. The percentage of points that overlay mitochondria (Mito), myofilaments (Myof), cytoplasm (Cyto) and lipid drops (LD) within the cells (excluding nuclei) was calculated, according to standard stereological methods.

Statistical analysis

Values are expressed as means ± S.E.M. Statistical significance of the difference between the different groups was estimated by one-way ANOVA using Newman–Keuls *post hoc* test. Values of $P < 0.05$ were considered significant.

Results

Anatomical characteristics and mouse heart myofibrillar function during postnatal development

Anatomical characteristics of the animals are presented in Table 1. Heart and body weight progressively increased until adulthood, whereas the heart weight to body weight ratio decreased after the age of 21 days. Maximal active tension at pCa 4.5 clearly increased during postnatal development until 21 days and then stabilized. Resting tension also increased during postnatal development. Myofibrillar calcium sensitivity was stable during development, while the Hill coefficient progressively increased.

Table 1. Anatomical parameters and myofibrillar function

Anatomical parameters	3 days	7 days	21 days	42 days	63 days
Number of animals	$N = 11$	$N = 15$	$N = 8$	$N = 5$	$N = 8$
Body weight (g)	$2.0 \pm 0.1^{***}$	$4.6 \pm 0.1^{***}$	$11.1 \pm 0.1^{***}$	$18.1 \pm 0.3^{***}$	24.4 ± 0.8
Heart weight (mg)	$12.7 \pm 0.3^{***}$	$29.8 \pm 0.7^{***}$	$75.2 \pm 1.2^{***}$	$110 \pm 3^{***}$	144 ± 4
Heart weight/body weight (mg g^{-1})	6.3 ± 0.1	$6.5 \pm 0.1^{*}$	$6.8 \pm 0.1^{***}$	6.1 ± 0.2	5.9 ± 0.1
Myofibrillar function	3 days	7 days	21 days	42 days	63 days
Number of fibres	$n = 4$	$n = 10$	$n = 10$	$n = 10$	$n = 9$
Resting tension (mN mm^{-2})	2.5 ± 0.6	3.3 ± 0.4	3.0 ± 0.4	4.3 ± 0.5	4.2 ± 0.4
Active tension (mN mm^{-2})	$9.4 \pm 0.7^{***}$	$16.8 \pm 1.2^{**}$	26.3 ± 1.9	29.5 ± 2.1	27.7 ± 1.9
pCa_{50}	5.97 ± 0.03	5.86 ± 0.03	5.91 ± 0.01	5.89 ± 0.01	5.92 ± 0.02
Hill coefficient	$2.64 \pm 0.5^{**}$	$2.82 \pm 0.3^{**}$	4.0 ± 0.3	4.3 ± 0.4	4.7 ± 0.4

Resting tension was recorded in the absence of calcium at a sarcomere length of 2.1 μm (20% stretch over the slack length). Active tension was recorded at maximal calcium concentration (pCa 4.5). pCa–tension relations were determined under isometric conditions by briefly placing each fibre into solutions of increasing calcium concentration until maximal tension was reached. Data were fitted using linearization of the Hill equation for relative tensions. pCa for half-maximal activation (pCa_{50}) and the Hill coefficient were calculated for each fibre by means of linear regression analysis. $^{*}P < 0.05$; $^{**}P < 0.01$; $^{***}P < 0.001$ *versus* adult (63 days).

Energetic support of sarcoplasmic reticulum ATPase

SR calcium content after 5 min of loading under the support of the different energy transfer pathways was measured in saponin-permeabilized muscle fibres (Fig. 2). The calcium content was assessed by measuring the force transient induced by SR calcium release following stimulation with caffeine. Maximal SR loading capacity was estimated under optimal energetic conditions, in the presence of exogenous ATP, PCr and working mitochondria. In 3-day-old mice, even under optimal conditions, calcium release could be detected in only a few muscle fibres (3 of 7), making the analysis of the data at this time point very difficult. This is nevertheless in line with the low level of expression of different SR proteins (SERCA, phospholamban and calsequestrin) at this stage of development (Fig. 3*A*). However, at 7 days after birth, significant Ca^{2+} release after loading under optimal energetic conditions (DANC+CK) could be detected (Fig. 2), indicative of SR maturation. At this age, DANC appeared to be as efficient as CK in supporting SR Ca^{2+} loading but less efficient than when both systems acted together ($P = 0.001$ for CK compared to optimal conditions) (Fig. 2). This apparent cooperation disappears later on in development. In the presence of CK and mitochondrial substrates, SR loading was significantly higher between day 7 and adulthood (Fig. 2), confirming that maturation of the SR was occurring (Fig. 3*A*); maximal loading was reached 21 days after birth. An increase in calcium uptake supported by creatine kinase alone matched this increase in SR loading capacity well, whereas SR Ca^{2+} loading in the presence of mitochondrial substrates did not increase further, indicating that at 7 days *post natum*, mitochondria were already maximally efficient at maintaining a high ATP/ADP ratio near SERCA. ATP alone was significantly less efficient than DANC or CK in supporting SR Ca^{2+} loading at all developmental stages, thus revealing the importance early on in development of both the DANC and CK pathways in SR energetic support.

Energetic support of myosin-ATPase

In the next experiment, we assessed the ability of the different energetic systems to support myosin-ATPase activity. To do this, we estimated the functional activity of myosin-ATPase under each of the different energetic conditions by measuring the rigor tension developed by fibres when the MgATP concentration was progressively decreased. The ability of DANC+CK and CK alone to support myosin-ATPase activity (in delaying the onset of

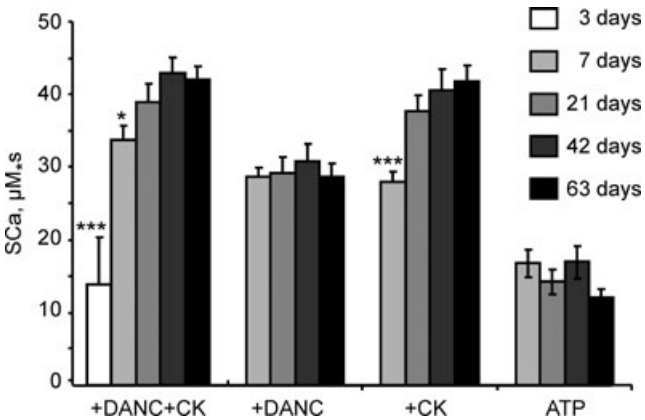

Figure 2. SR calcium loading under different energetic conditions in permeabilized cardiac fibres at different ages
Calcium uptake at pCa 6.5 in the presence of different ATP sources: external (ATP), and endogenous, namely bound CK (+CK), mitochondria (+DANC) or both (+DANC+CK). By relating the subsequent contractile force elicited with caffeine to the calcium–force curve for each fibre, the $[Ca^{2+}]$–time integral (SCa) was calculated as an index of SR calcium load. $n = 7$–10 fibres from 3–7 animals for each age. $^{*}P < 0.05$, $^{***}P < 0.001$ *versus* adult age (63 days).

rigor) was similar for all ages (Fig. 4). However, when energetic support was provided by DANC only, rigor tension appeared significantly earlier in 3-day-old muscle fibres than in older fibres ($pMgATP_{50}$: 4.03 ± 0.02 and 4.36 ± 0.07 in 3- and 7-day-old muscle fibres respectively, $P < 0.01$). Thus, the mitochondrial energy supply was not yet mature in 3-day-old mice. These results indicate that bound-CK could regulate the ATP/ADP ratio near myosin-ATPase as early as 3 days *post natum* whereas mitochondrial DANC support for the myofibrils matured later. Note that this period between 3 and 7 days after birth is marked by an increase in the α-MHC/β-MHC ratio (Fig. 3*B*).

One possible explanation for the emergence of mature mitochondrial DANC between the ages of 3 and 7 days is that mitochondrial function perhaps increased during this short period. Another explanation may be that changes in cardiomyocyte architecture occurred which helped improve the energetic crosstalk between mitochondria and myosin-ATPase.

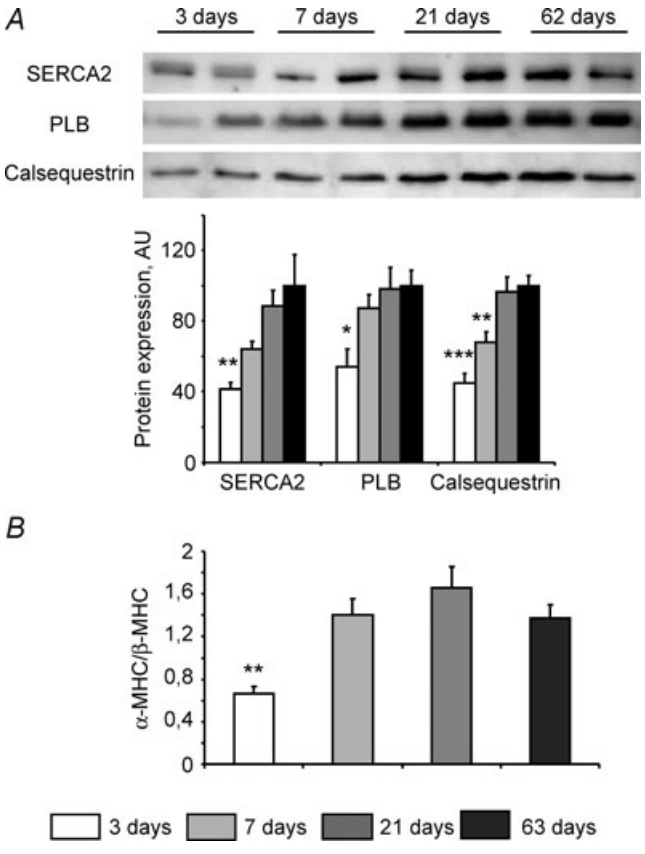

Figure 3. Molecular characterization of the heart at different ages
A, Western blot analysis of SERCA2, phospholamban (PLB) and calsequestrin expression at different ages. Upper panel: representative original recording. Lower panel: mean values of protein content ($n = 8$ for each age). *B*, ratio of α-MHC to β-MHC mRNA expression measured by real-time quantitative RT-PCR. $N = 8$ animals for each age. $^{*}P < 0.05$, $^{**}P < 0.01$, $^{***}P < 0.001$ *versus* adult age (63 days).

Evolution of the intrinsic parameters of energy metabolism

In the next experiment, we studied whether the differences in DANC and CK efficacy are linked to differences in the intrinsic activity of mitochondria and CK during postnatal development. The rate of mitochondrial oxygen consumption was measured in saponin-permeabilized muscle fibres. Respiration rates in the absence (V_0, basal respiration) or in the presence (V_{max}, maximal respiration) of a saturating ADP concentration increased progressively during postnatal development. A 332% increase in V_{max} was observed between 3 and 63 days of age (Fig. 5*A*). However, V_{max} values measured in the 3- and 7-day-old mice were not significantly different (4.5 ± 0.6 and 5.9 ± 0.6 μmol O_2 min^{-1} (g dry weight)$^{-1}$, respectively, $P = 0.33$). As the evolution of V_0 during postnatal development followed that of V_{max}, the acceptor control ratio (ACR) therefore remained constant (Fig. 5*B*). Mitochondrial content, estimated by measuring citrate synthase activity, a marker of the mitochondrial mass (Fig. 5*C*), was significantly greater in adult heart than in 3-day- or 7-day-old hearts. Similarly, Complex I activity was also considerably higher in older mice (Fig. 5*D*). The difference in estimated mitochondrial content between 3 and 7 days was not statistically significant (497 ± 63 and 564 ± 39 UI (g protein)$^{-1}$, respectively, $P = 0.31$), suggesting that cardiac mitochondrial content did not increase between these ages. The only parameter that was statistically different between these two ages was Complex I activity (Fig. 5*D*), which had increased by 7 days of age

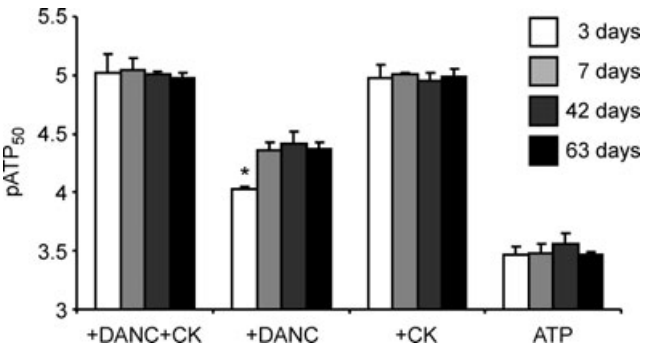

Figure 4. Sensitivity of rigor tension to MgATP from different sources in 3-, 7-, 42- and 63-day-old mice
$pMgATP_{50}$ (pMgATP for half-maximal rigor tension) and role of creatine kinase and/or mitochondria in myofibrillar-ATPase energy supply. Rigor tension was recorded in solutions of decreasing MgATP concentration using different solutions that control ATP sources: external (ATP), and endogenous, namely bound CK (+CK), mitochondria (+DANC) or both (+DANC+CK). $n = 6$–11 fibres from 3–6 animals for each age. $pMgATP_{50}$: $^{*}P < 0.05$ *vs*. 63 days.

and which increased further in older mice. In general, these results suggest that the emergence between 3 and 7 days of age of efficient mitochondrial direct ATP channelling to myosin-ATPase was not, in fact, the consequence either of a marked difference in mitochondrial content or in the intrinsic function of mitochondria.

Interestingly, in contrast to the maturation of oxidative capacity, mitochondrial sensitivity to ADP (estimated using the Michaelis constant) did not change during early development (Fig. 5*E*). In adult animals, whilst the K_m in the presence of creatine was not changed, ADP sensitivity in the absence of creatine showed a spectacular decrease (K_m was augmented from 87 ± 17 in 21-day-old mice to 226 ± 31 μmol l^{-1} in 63-day-old mice), indicating that the functional activity of mitochondrial CK was markedly higher in adult myocardium (Fig. 5*F*). This evolution in CK function did not, however, correlate with developmental changes in mitochondrial CK expression, which increased rather early (up to 7 days of age) before stabilizing (Fig. 5*G*). Total CK activity in ventricular tissue (Fig. 5*H*) showed a progressive increase from 3 days *post natum* up to adult age.

Cardiomyocyte ultrastructure and mitochondrial network organization during development

Since the functional analysis of mitochondria did not reveal why the efficacy of DANC between mitochondria and myosin-ATPase was lower in 3-day-old than 7-day-old mice, we looked instead for changes in cardiomyocyte ultrastructure during this period. Electron microscopy showed that at 3 days *post natum* there was a large amount of cytosolic space in the centre of cardiomyocytes, with the myofibrils situated at the periphery of the cell. The myofibrils were oriented parallel to the longitudinal axis of the cells with the mitochondria clustered in the cytosol predominantly around the nuclei (Fig. 6*A*). Clearly, in 3-day-old mouse hearts the mitochondrial network was not well organized and intermyofibrillar mitochondria were irregularly dispersed and not aligned (Fig. 6*A*). Thus, in the youngest mice mitochondria and myofilaments did not show obvious signs of having a mature organisation. By contrast, 7-day-old cardiomyocytes had a substantially less cytoplasmic space (Fig. 6*B*) and were predominantly filled with clusters of mitochondria arranged along longitudinally oriented myofilaments. Twenty-one days after birth, the ultrastructure of cardiomyocytes was regular, the interior of the cells was filled with myofibrils, and mitochondria were aligned in the longitudinal direction, similar to the appearance of adult cells (Fig. 6*C* and *D*).

Another striking difference among myocytes of different ages was in mutual spatial interaction among mitochondria, sarcoplasmic reticulum and myofibrils. While in 3-day-old myocytes the mitochondria and the sarcoplasmic reticulum are freely distributed in the cytoplasm around myofibrils (Fig. 7*A*), at later stages of myocyte maturation, there is obvious increase in direct contacts between mitochondria and myofibrils. Indeed, mitochondria and myofilaments were separated by a large cytosolic space in the cells of the youngest mice (Fig. 7*A*), which greatly decreased at 7 days of age (Fig. 7*B*). This means that from 7 days of age mitochondria were closer to myosin-ATPase than in the 3-day-old mice. This

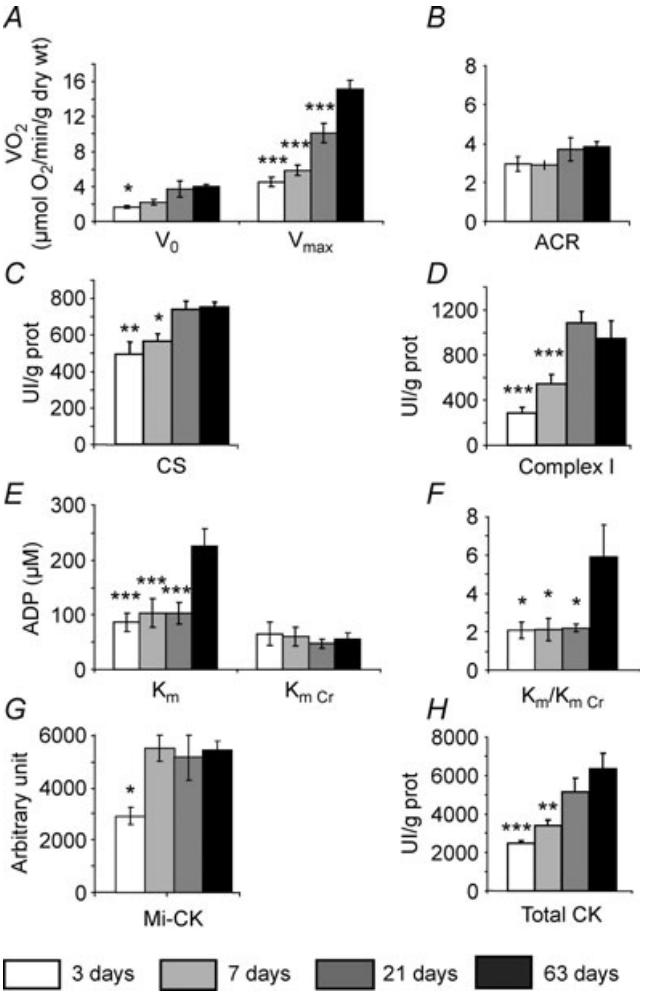

Figure 5. Intrinsic energy metabolism parameters at different ages
A, oxidative capacities of ventricular fibres were measured in the presence of 2 mM ADP, at saturating concentration of substrates. ($n = 15$ fibre bundles from 5–9 animals for each age.) *B*, acceptor control ratio was calculated as the ratio between maximal respiration rate (V_{max}) and basal respiration rate (V_0). *C*, citrate synthase (CS) enzymatic activity. *D*, Complex I enzymatic activity. *E*, apparent K_m of mitochondrial consumption for ADP without or with 12 mM creatine. *F*, ratio between K_m without creatine and K_m with creatine. *G*, Mi-CK expression. *H*, total CK activity. ($N = 8$ animals for each age.) $^*P < 0.05$, $^{**}P < 0.01$, $^{***}P < 0.001$ *versus* 63 days.

could explain the difference in DANC efficiency between these two ages. In general, mitochondria-myofilament organization at the age of 7 days was more similar to the organization of older cells (Fig. 7*C* and *D*) than the organization of 3-day-old mice.

The biochemical and functional data indicated that there was not much SR at 3 days after birth. Indeed, sarcoplasmic reticulum could only be seen occasionally (Fig. 8*A*). By contrast, in 7-day-old cardiomyocytes the SR was developed. The longitudinal SR displayed short profiles and chains of vesicles near the myofibrils (Fig. 8*B*). Older cells (21 days and 63 days) clearly showed mature longitudinal SR and t-tubules forming dyads near Z-lines (Fig. 8*C* and *D*).

Maturation process of the ultrastructure was not homogeneous. This is confirmed by stereological quantification of changes in volume densities of major organelles (Fig. 9). Comparison of changes in volume densities reveals earlier maturation of the mitochondrial content compared to the content of myofibrils. Of note is the drastic decrease in the cytosol content between 3 and 7 days and the peak of lipid drops content at the 7 day.

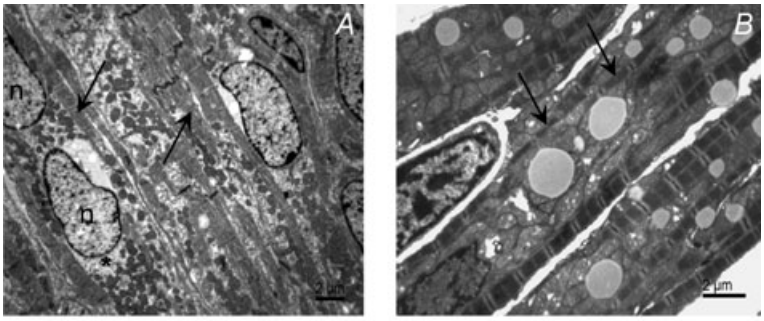

Figure 6. Electron micrographs of cardiomyocytes of papillary muscle
A, 3-day-old cardiomyocytes having a high content of free cytoplasm, myofibrils situated under the plasma membrane (arrows) and mitochondria clustered in the perinuclear regions (*). *B*, 7-day-old cardiomyocytes showing abundant mitochondrial clusters, and myofilaments of small diameters (arrows). *C*, 21-day-old cardiomyocytes showing regularly arranged myofilaments and mitochondria aligned in the longitudinal direction. *D*, 63-day-old cardiomyocytes demonstrating regular overall ultrastructure. Myofilaments and mitochondria are arranged in parallel along the longitudinal axis.

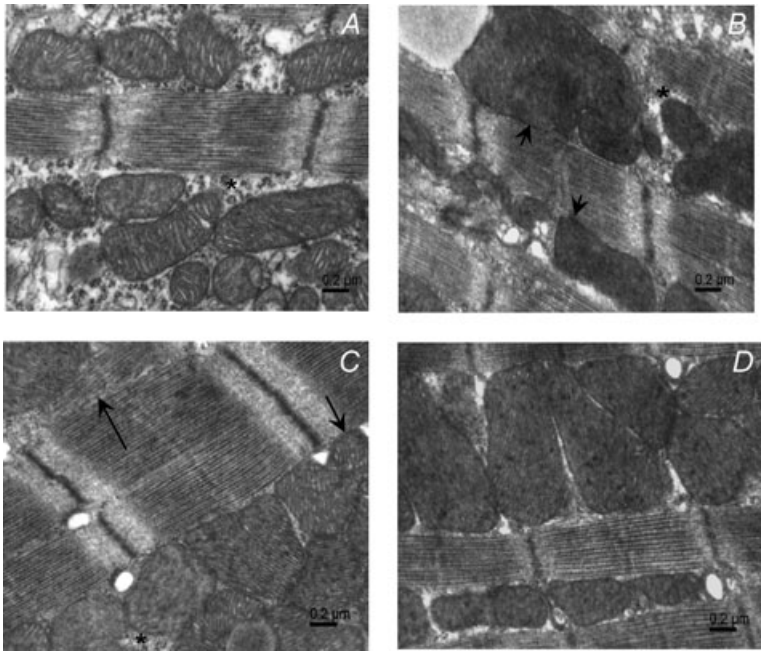

Figure 7. Spatial interaction between mitochondria and myofilaments in developing cardiomyocytes
A, 3-day-old cardiomyocytes with large cytoplasmic space (*) between myofilaments and mitochondria which are not in tight contact to each other. *B*, 7-day-old cardiomyocytes showing mitochondria in direct contact with myofilaments (short arrows) even though a thin layer of cytoplasm can still be found between mitochondria and myofibrils (*). *C*, 21-day-old cardiomyocytes with well developed longitudinal SR (arrow) and mitochondria in close contact with the myofibrils (short arrow). *D*, 63-day-old cardiomyocytes with mitochondria in direct contact with myofilaments.

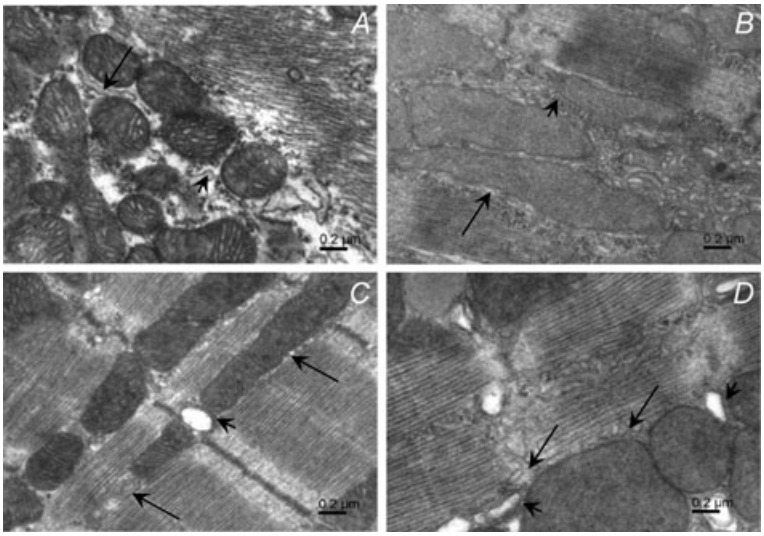

Figure 8. Electron micrographs of cardiomyocytes showing spatial relationship of mitochondria and sarcoplasmic reticulum
A, mitochondrial cluster in 3-day-old mice cardiomyocytes. Profiles of rough endoplasmic reticulum (short arrow) and short stretches of sarcoplasmic reticulum (arrow) are present between mitochondria. *B*, 7-day-old cardiomyocytes show the presence of longitudinal sarcoplasmic reticulum between the myofilaments and the mitochondrial surface (arrow). Occasionally, short stretches of rough endoplasmic reticulum near the mitochondria are still observed (short arrow). *C*, 21-day-old cardiomyocytes with well developed longitudinal sarcoplasmic reticulum (arrows). The cisternae of SR of the dyads occur in the close vicinity of the mitochondrial surface (short arrow). *D*, 63-day-old cardiomyocytes display a rich network of sarcoplasmic reticulum (arrows) and cisternae of SR (short arrow) close to mitochondria.

Discussion

In the present study, we investigated the formation of intracellular energetic pathways during the hypertrophic phase of postnatal development of the mouse heart. We correlated the efficacy of energy transfer by DANC and CK with the degree of cell organization and organelle function. The main finding is that maturation of these two pathways is not simultaneous. Unexpectedly, we found that DANC was as efficient at regulating local SR and myosin-ATPase function from 7 days *post natum* as it was in adult cardiomyocytes, despite there being a non-maximal respiration capacity. By contrast, CK efficacy for acto-myosin ATPase regulation was maximal from 3 days *post natum*, whereas for SR ATPase regulation it progressively increased until 21 days *post natum*. Importantly, between 3 and 7 days after birth, we saw major cytoarchitectural remodelling, which is probably crucial to the improvement in energy transfer between mitochondria and myosin-ATPase. Our results highlight the complex relationship between energetics, architecture and cell function, and the need for very early optimization of local energy regulation.

Postnatal development as a model of physiological hypertrophy

Postnatal development offers a unique opportunity to understand the physiological importance of cell architecture and mitochondrial network organization in mammalian cardiac cell. If early postnatal growth is achieved by hyperplasia, very rapidly (3 days after birth in the mouse heart; see Leu *et al.* 2001) a second phase occurs involving hypertrophy of the cardiomyocyte. It is during this hypertrophic phase that the complex structures involved in excitation–contraction coupling like SR or T tubules develop, providing the cardiomyocyte with a compartmented Ca^{2+} handling system and efficient amplification of the calcium signal.

Based on the results obtained in this study, the period between 3 and 7 days after birth appears to be an important step in the building up of mitochondria–SR and mitochondria–myofibril contacts in mouse cardiomyocytes. It is also during this period that SR and T-tubules organization is built up for maximum excitation–contraction coupling efficiency. Thus, it seems probable that this is during this short period of time that mitochondria, myofibrils and SR acquire their fixed position to form an effective intracellular energetic unit.

Interestingly, after 7 days, even if some modifications still occur, the whole cytoarchitecture organization seems

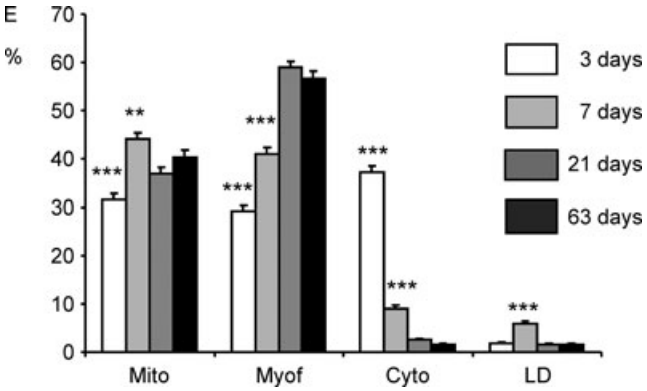

Figure 9. Stereological measurements of cardiomyocytes of papillary muscles
Relative cell volume occupied by mitochondria (Mito), myofilaments (Myof), cytosol (Cyto) and lipids drops (LD), evaluated from 20 images taken from 2 hearts of animals for each age. $^{**}P < 0.01$, $^{***}P < 0.001$ *versus* 63 days.

to be almost completed. The major changes observed between 7 and 21 days is a further increase in the myofilament compartment at the expense of the cytosol. It means that after this period, there is probably another type of hypertrophy where no major remodelling of the contacts between organelles occurs.

In parallel, compartmentation of the CK system contributes to cell maturation and the development of a sophisticated pathway of energy transfer from sites of energy production to sites of utilization (Hoerter *et al.* 1994; Tiivel *et al.* 2000). The mitochondrial network also undergoes profound remodelling. Mitochondria appear as isolated ellipsoids or tubules in embryonic stages but then reorganize into a reticular network in the adult heart (Muhlfeld *et al.* 2006). Moreover, mitochondrial volume increases and mitochondria exhibit morphological remodelling, causing changes in mitochondrial regulation and the formation of restricted diffusion domains (Anmann *et al.* 2006).

Our results show that the maturation of oxidative capacities is a rather long process. Despite the fact that major mitochondria network modifications are already visible by 21 days, there is a large increase of maximal respiration capacity (V_{max}), suggesting the presence of more active mitochondria in adult heart. Perhaps more importantly, after 21 days, the access of external ADP to mitochondria becomes much more limited, which could be evidenced by a dramatic rise in the apparent K_m for ADP. This indicates appearance of a new energetic microdomain in the mitochondrial cellular compartment that needs mitochondrial CK to ensure adenine nucleotide exchange with extramitochondrial compartments. This long-lasting process of maturation of the mitochondrial sensitivity to ADP may also be related to development of various systems controlling ADP accessibility, for example adenine nucleotide translocase (ANT), in particular, isoform ANT1, which shows relatively slow maturation (Skarka *et al.* 2003). The time course of development of voltage-dependent anion channels (VDACs) or tubulin-related structures, which seem to be involved in the regulation of adenine nucleotide fluxes (Timohhina *et al.* 2009), might also determine such a maturation.

Lastly, the appearance of cell crowding and dense cytoarchitecture of the adult cardiomyocyte is well evidenced by the drastic decrease of the cytosolic compartment from $37.3 \pm 1.3\%$ at 3 days to $1.6 \pm 0.3\%$ in the adult.

Interestingly, between 21 days and 2 months there is a marked decrease in heart weight to body weight ratio. This suggests that the previous setting of all compartments and organisation of mitochondrial network allow cardiomyocytes to increase their contractile and metabolic efficiency, despite no major modification of cyto-architecture arrangement.

Local regulation of energy-handling in the vicinity of ATPases during development

An important finding of this study is that energetic microdomains are established very early in the development of the mouse heart. Already by 3 days *post natum*, both DANC and CK regulate the ATP/ADP ratio near myosin ATPase much more effectively than simple adenine nucleotide diffusion. This is probably a very important developmental change, because the cardiomyocyte cytosol rapidly becomes densely packed and diffusion between organelles limited. At 3 days *post natum*, MM-CK appears to be at its maximal capacity in supporting myosin ATPase function. Moreover, energetic compartmentation in the mouse heart appears earlier than in the rat (Hoerter *et al.* 1994) or rabbit heart, in which the CK system is not very efficient until at least 8 days *post natum* (Hoerter *et al.* 1991), but it appears later than in the guinea pig where the CK system is already compartmented before birth (Hoerter *et al.* 1994). In contrast, we found that CK bound close to SERCA in mouse cardiomyocytes becomes maximally efficient only after 3 weeks of age. Thus bound CK in the vicinity of myofibrillar-ATPase becomes more efficient much earlier than bound CK in the vicinity of SERCA, even though the same CK isoform (MM-CK) is involved (Rossi *et al.* 1990; Wallimann & Eppenberger 1985). It would therefore seem that CK is preferentially localized near the myofilaments at the beginning of life *post natum* in the mouse.

Efficient direct energy transfer from mitochondria to myosin ATPase appears to be dependent on the cytoarchitecture, in contrast to the CK-supported energy transfer, which seems mainly to depend on enzyme expression and specific localisation. Indeed, we observed a significant improvement in the local regulation of myosin ATPase by mitochondria between 3 and 7 days after birth, despite unchanged maximal respiration capacity of mitochondria and myofilament to mitochondria ratio (Fig. 9), and an increase in myofilament energy demand evidenced by an increasing proportion of α-MHC isoform having the highest ATPase activity (Schiaffino & Reggiani 1996). It is during this period that major cytoarchitectural modifications are seen; the cytosolic space drastically diminishes, and the cells become densely packed and filled with clusters of mitochondria in close proximity to longitudinally oriented myofibrils (Figs 6 and 8) leading to restricted diffusion in the cytosol (Saks *et al.* 1991).

The close contact between mitochondria and SR occurs very early in development and in parallel with maturation of the SR. In our study, the absence of calcium release in several 3-day-old fibres could have been due to immaturity of the SR consisted with the low expression of SERCA2 in the youngest mice. Indeed, at 3 days of age, SR density is very low with little SR maturation visible. As a matter of fact, the contraction of very young cardiomyocytes is less

dependent on SR calcium release but highly dependent on transarcolemmal Ca^{2+} influx (Tanaka *et al.* 1998; Schroder *et al.* 2006). In 7-day-old mice, by contrast, the SR could easily be seen and functionally reached about 80% of the adult capacity. More importantly, it was as efficiently coupled to mitochondria as in adult heart.

In conclusion, we have shown in this paper the early formation of energetic micro-domains during the postnatal development of the mouse heart, and the need for the maturation of cell architecture to achieve maximal efficacy of mitochondria for the regulation of ATPases. We think that postnatal development constitutes a good model for understanding the role of energetic and of cytoarchitecture in the optimization of cardiac function.

References

Anmann T, Guzun R, Beraud N, Pelloux S, Kuznetsov AV, Kogerman L, Kaambre T, Sikk P, Paju K, Peet N, Seppet E, Ojeda C, Tourneur Y & Saks V (2006). Different kinetics of the regulation of respiration in permeabilized cardiomyocytes and in HL-1 cardiac cells. Importance of cell structure/organization for respiration regulation. *Biochim Biophys Acta* **1757**, 1597–1606.

De Sousa E, Veksler V, Minajeva A, Kaasik A, Mateo P, Mayoux E, Hoerter J, Bigard X, Serrurier B & Ventura-Clapier R (1999). Subcellular creatine kinase alterations. Implications in heart failure. *Circ Res* **85**, 68–76.

Estornell E, Fato R, Pallotti F & Lenaz G (1993). Assay conditions for the mitochondrial NADH:coenzyme Q oxidoreductase. *FEBS Lett* **332**, 127–131.

Garnier A, Fortin D, Delomenie C, Momken I, Veksler V & Ventura-Clapier R (2003). Depressed mitochondrial transcription factors and oxidative capacity in rat failing cardiac and skeletal muscles. *J Physiol* **551**, 491–501.

Hew KW & Keller KA (2003). Postnatal anatomical and functional development of the heart: a species comparison. *Birth Defects Res B Dev Reprod Toxicol* **68**, 309–320.

Hoerter JA, Kuznetsov A & Ventura-Clapier R (1991). Functional development of the creatine kinase system in perinatal rabbit heart. *Circ Res* **69**, 665–676.

Hoerter JA, Ventura-Clapier R & Kuznetsov A (1994). Compartmentation of creatine kinases during perinatal development of mammalian heart. *Mol Cell Biochem* **133–134**, 277–286.

Kaasik A, Veksler V, Boehm E, Novotova M, Minajeva A & Ventura-Clapier R (2001). Energetic crosstalk between organelles: architectural integration of energy production and utilization. *Circ Res* **89**, 153–159.

Kuznetsov AV, Veksler V, Gellerich FN, Saks V, Margreiter R & Kunz WS (2008). Analysis of mitochondrial function in situ in permeabilized muscle fibres, tissues and cells. *Nat Protoc* **3**, 965–976.

Leu M, Ehler E & Perriard JC (2001). Characterisation of postnatal growth of the murine heart. *Anat Embryol (Berl)* **204**, 217–224.

Minajeva A, Ventura-Clapier R & Veksler V (1996). Ca^{2+} uptake by cardiac sarcoplasmic reticulum ATPase in situ strongly depends on bound creatine kinase. *Pflugers Arch* **432**, 904–912.

Muhlfeld C, Urru M, Rumelin R, Mirzaie M, Schondube F, Richter J & Dorge H (2006). Myocardial ischemia tolerance in the newborn rat involving opioid receptors and mitochondrial K^+ channels. *Anat Rec A Discov Mol Cell Evol Biol* **288**, 297–303.

Ogata T & Yamasaki Y (1985). Scanning electron-microscopic studies on the three-dimensional structure of mitochondria in the mammalian red, white and intermediate muscle fibres. *Cell Tissue Res* **241**, 251–256.

Ostadal B, Ostadalova I & Dhalla NS (1999). Development of cardiac sensitivity to oxygen deficiency: comparative and ontogenetic aspects. *Physiol Rev* **79**, 635–659.

Rossi AM, Eppenberger HM, Volpe P, Cotrufo R & Wallimann T (1990). Muscle-type MM creatine kinase is specifically bound to sarcoplasmic reticulum and can support Ca^{2+} uptake and regulate local ATP/ADP ratios. *J Biol Chem* **265**, 5258–5266.

Saks VA, Belikova YO & Kuznetsov AV (1991). In vivo regulation of mitochondrial respiration in cardiomyocytes: specific restrictions for intracellular diffusion of ADP. *Biochim Biophys Acta* **1074**, 302–311.

Saks VA, Kaambre T, Sikk P, Eimre M, Orlova E, Paju K, Piirsoo A, Appaix F, Kay L, Regitz-Zagrosek V, Fleck E & Seppet E (2001). Intracellular energetic units in red muscle cells. *Biochem J* **356**, 643–657.

Saks VA, Khuchua ZA, Vasilyeva EV, Belikova OYu & Kuznetsov AV (1994). Metabolic compartmentation and substrate channelling in muscle cells. Role of coupled creatine kinases in in vivo regulation of cellular respiration: a synthesis. *Mol Cell Biochem* **133–134**, 155–192.

Schiaffino S & Reggiani C (1996). Molecular diversity of myofibrillar proteins: gene regulation and functional significance. *Physiol Rev* **76**, 371–423.

Schroder EA, Wei Y & Satin J (2006). The developing cardiac myocyte: maturation of excitability and excitation-contraction coupling. *Ann N Y Acad Sci* **1080**, 63–75.

Seppet EK, Eimre M, Anmann T, Seppet E, Peet N, Kaambre T, Paju K, Piirsoo A, Kuznetsov AV, Vendelin M, Gellerich FN, Zierz S & Saks VA (2005). Intracellular energetic units in healthy and diseased hearts. *Exp Clin Cardiol* **10**, 173–183.

Seppet EK, Kaambre T, Sikk P, Tiivel T, Vija H, Tonkonogi M, Sahlin K, Kay L, Appaix F, Braun U, Eimre M & Saks VA (2001). Functional complexes of mitochondria with Ca,MgATPases of myofibrils and sarcoplasmic reticulum in muscle cells. *Biochim Biophys Acta* **1504**, 379–395.

Skarka L, Bardova K, Brauner P, Flachs P, Jarkovska D, Kopecky J & Ostadal B (2003). Expression of mitochondrial uncoupling protein 3 and adenine nucleotide translocase 1 genes in developing rat heart: putative involvement in control of mitochondrial membrane potential. *J Mol Cell Cardiol* **35**, 321–330.

Tanaka H, Sekine T, Nishimaru K & Shigenobu K (1998). Role of sarcoplasmic reticulum in myocardial contraction of neonatal and adult mice. *Comp Biochem Physiol A Mol Integr Physiol* **120**, 431–438.

Tiivel T, Kadaya L, Kuznetsov A, Kaambre T, Peet N, Sikk P, Braun U, Ventura-Clapier R, Saks V & Seppet EK (2000). Developmental changes in regulation of mitochondrial respiration by ADP and creatine in rat heart in vivo. *Mol Cell Biochem* **208**, 119–128.

Timohhina N, Guzun R, Tepp K, Monge C, Varikmaa M, Vija H, Sikk P, Kaambre T, Sackett D & Saks V (2009). Direct measurement of energy fluxes from mitochondria into cytoplasm in permeabilized cardiac cells in situ: some evidence for mitochondrial interactosome. *J Bioenerg Biomembr* **41**, 259–275.

Vandesompele J, De Preter K, Pattyn F, Poppe B, Van Roy N, De Paepe A & Speleman F (2002). Accurate normalization of real-time quantitative RT-PCR data by geometric averaging of multiple internal control genes. *Genome Biol* **3**, research0034.1-0034.II.

Veksler VI, Kuznetsov AV, Anflous K, Mateo P, van Deursen J, Wieringa B & Ventura-Clapier R (1995). Muscle creatine kinase-deficient mice. II. Cardiac and skeletal muscles exhibit tissue-specific adaptation of the mitochondrial function. *J Biol Chem* **270**, 19921–19929.

Veksler VI, Kuznetsov AV, Sharov VG, Kapelko VI & Saks VA (1987). Mitochondrial respiratory parameters in cardiac tissue: a novel method of assessment by using saponin-skinned fibres. *Biochim Biophys Acta* **892**, 191–196.

Ventura-Clapier R, Kuznetsov A, Veksler V, Boehm E & Anflous K (1998). Functional coupling of creatine kinases in muscles: species and tissue specificity. *Mol Cell Biochem* **184**, 231–247.

Ventura-Clapier R, Kuznetsov AV, d'Albis A, van Deursen J, Wieringa B & Veksler VI (1995). Muscle creatine kinase-deficient mice. I. Alterations in myofibrillar function. *J Biol Chem* **270**, 19914–19920.

Ventura-Clapier R & Veksler V (1994). Myocardial ischemic contracture. Metabolites affect rigor tension development and stiffness. *Circ Res* **74**, 920–929.

Wallimann T & Eppenberger HM (1985). Localization and function of M-line-bound creatine kinase. M-band model and creatine phosphate shuttle. *Cell Muscle Motil* **6**, 239–285.

Wallimann T, Wyss M, Brdiczka D, Nicolay K & Eppenberger HM (1992). Intracellular compartmentation, structure and function of creatine kinase isoenzymes in tissues with high and fluctuating energy demands: the 'phosphocreatine circuit' for cellular energy homeostasis. *Biochem J* **281**, 21–40.

Wharton DC & Tzagoloff A (1967). Cytochrome oxidase from beef heart mitochondria. *Methods Enzymol* **10**, 245–250.

Wilding JR, Joubert F, de Araujo C, Fortin D, Novotova M, Veksler V & Ventura-Clapier R (2006). Altered energy transfer from mitochondria to sarcoplasmic reticulum after cytoarchitectural perturbations in mice hearts. *J Physiol* **575**, 191–200.

Author contributions

J.P. carried out the major part of the experimental work. M.N. performed and commented on images of electron microscopy (in the Slovak Republic). D.F. measured enzyme activities and prepared tissues for electron microscopy analysis. A.G. carried out real-time quantitative PCR experiment. All authors were involved in study design, data analysis and interpretation. J.P., M.N, R.V.-C., V.V. and F.J. wrote the paper and contributed to figure preparation. All authors discussed the results, commented on the manuscript and approved the version to be published.

Acknowledgements

This work was in part supported by a grant VEGA 2/0174/09. We thank Dr R. Fischmeister for continuous support and Dr J. Wilding for careful reading of the manuscript. We also thank Valérie Domergue-Dupont and the animal care facility of IFR141 for efficient handling and preparation of the animals. In addition, we thank Ladislav Novota for skilful technical assistance. This work was supported by grants from the European Union contract LSHM-CT-2005-018833/EUGeneHeart. R.V.-C. and F.J. are scientists at Centre National de la Recherche Scientifique.